

Edinburgh 2006/13  
LAPTH-1154/06  
June 2006

# New one-loop techniques and first applications to LHC phenomenology

T. Binoth<sup>a</sup>, A. Guffanti<sup>a</sup>, J.-Ph. Guillet<sup>b</sup>, S. Karg<sup>c</sup>, N. Kauer<sup>c</sup> and T. Reiter<sup>a</sup>

<sup>a</sup>School of Physics, SUPA, The University of Edinburgh,  
Mayfield Road, Edinburgh EH9 3JZ, Scotland, UK.

<sup>b</sup>Laboratoire d'Annecy-le-Vieux de Physique Théorique LAPTH,  
B.P. 110, F-74941 Annecy-le-Vieux Cedex, France.

<sup>c</sup>Faculty for Theoretical Physics, University of Wuerzburg,  
Am Hubland, D-97074 Wuerzburg, Germany.

In this talk we describe our approach for the computation of multi-leg one-loop amplitudes and present some first results relevant for LHC phenomenology.

## 1. Motivation

In the next year the Large Hadron Collider at CERN will start operating at the up to now unreached TeV energy scale. Apart from putting our theoretical understanding of the electroweak symmetry breaking mechanism under scrutiny, new effects beyond the Standard Model that occur in this energy region can also be explored [1,2]. A successful quantitative analysis and comparison of the LHC data with theoretical predictions will crucially rely not only on precise predictions for a variety of signal cross sections, but also on a sufficiently precise knowledge of the various backgrounds. Although in some favourable cases the Standard Model backgrounds can be measured directly, for other important search channels this is not possible and backgrounds have to be determined through theoretical predictions. This is especially worrisome, as QCD predictions for multi-particle processes are plagued by large uncertainties arising from high powers of  $\alpha_s$ . Large scale uncertainties make it mandatory to include radiative corrections beyond the leading order in QCD. Unfortunately, due to the complicated singularity structure of QCD and the general combinatorial complexity of multi-scale problems, one-loop computations with more than four external partons/particles are a highly non-

trivial and time-consuming task. Fortunately, at the dawn of the LHC era, this research direction is very actively pursued by multiple groups [3,4,5,6,7,8,9,10,11,12,13,14].

In this talk I present our approach to this problem. The aim of our collaboration is to build a flexible and reliable tool, which allows for the evaluation of one-loop multi-leg amplitudes. It is based on a combination of algebraic and numerical methods. The corresponding project is called GOLEM (General One-Loop Evaluator for Matrix elements) and will be discussed in the next section. Section 3 is dedicated to first applications of these methods relevant for LHC phenomenology.

## 2. The GOLEM project

A General One-Loop Evaluator for Matrix elements (GOLEM) should proceed from a Feynman diagrammatic representation of a given scattering amplitude to a computer code which provides a numerically stable and accurate answer for the desired cross section.

In a first step each amplitude can be represented in terms of irreducible Lorentz tensors which correspond uniquely to gauge invariant operators:

$$\mathcal{A}(|p_j\rangle, \epsilon_j^\lambda, \dots) = \sum_I \mathcal{A}_I(|p_j\rangle, \epsilon_j^\lambda, \dots) .$$

The mapping of the diagrammatic input onto such a tensorial basis can be accomplished with algebraic manipulation programs. We generally use FORM 3.1 [15]. Each Feynman diagram  $\mathcal{G}_G$  can be projected onto these sub-amplitudes:

$$\begin{aligned} \mathcal{A}(|p_j\rangle, \epsilon_j^\lambda, \dots) &= \sum_G \mathcal{G}_G(|p_j\rangle, \epsilon_j^\lambda, \dots) \\ &= \sum_I \sum_G \mathcal{C}_{IG}(s_{jk}) \mathcal{T}_I(|p_j\rangle, \epsilon_j^\lambda, \dots) \quad . \end{aligned}$$

The coefficients  $\mathcal{C}$  of the gauge invariant operators are momentum space integrals where free Lorentz indices are contracted with external momentum vectors. In a third step these coefficients, which depend on Mandelstam variables  $s_{ij} = (p_i + p_j)^2$  only, are expressed in terms of some integral basis to be discussed below:

$$\begin{aligned} \mathcal{A}(|p_j\rangle, \epsilon_j^\lambda, \dots) &= \sum_{BIG} \mathcal{C}_{BIG}(s_{jk}, \dots) \\ &\quad \times I_B \mathcal{T}_I(|p_j\rangle, \epsilon_j^\lambda, \dots) \quad . \end{aligned}$$

In a forth step, the coefficients have to be exported to some numerical programming language. Optionally they can be simplified beforehand using algebraic programs like MAPLE or MATHEMATICA:

$$\begin{aligned} \mathcal{A}(|p_j\rangle, \epsilon_j^\lambda, \dots) &= \sum_{BIG} I_B \mathcal{T}_I(|p_j\rangle, \epsilon_j^\lambda, \dots) \\ &\quad \times \text{simplify}[\mathcal{C}_{BIG}(s_{jk}, \dots)] \quad . \end{aligned}$$

We now discuss the integral basis used for our reduction algorithms. Following [16] one can represent any given tensor integral by Feynman parameter integrals in shifted dimensions:

$$\begin{aligned} I_N^{\mu_1 \dots \mu_R} &= \sum \tau^{\mu_1 \dots \mu_R}(r_{j_1}, \dots, r_{j_r}, g^m) \\ &\quad \times I_N^{n+2m}(j_1, \dots, j_r) \quad . \end{aligned}$$

By applying differentiation by parts in parameter space and  $d = 4$  kinematical identities [7] one can map all these integrals to the following basis without the need for higher dimensional scalar integrals with  $N > 4$ :

$$\begin{aligned} I_3^n(j_1, \dots, j_r) &= -\Gamma\left(3 - \frac{n}{2}\right) \\ &\times \int_0^1 \prod_{i=1}^3 dz_i \frac{z_{j_1} \dots z_{j_r} \delta(1 - \sum_{l=1}^3 z_l)}{(-\frac{1}{2} z \cdot \mathcal{S} \cdot z)^{3-n/2}} \quad , \end{aligned}$$

$$\begin{aligned} I_3^{n+2}(j_1) &= -\Gamma\left(2 - \frac{n}{2}\right) \\ &\times \int_0^1 \prod_{i=1}^3 dz_i \frac{z_{j_1} \delta(1 - \sum_{l=1}^3 z_l)}{(-\frac{1}{2} z \cdot \mathcal{S} \cdot z)^{2-n/2}} \quad , \\ I_4^{n+2}(j_1, \dots, j_r) &= \Gamma\left(3 - \frac{n}{2}\right) \\ &\times \int_0^1 \prod_{i=1}^4 dz_i \frac{z_{j_1} \dots z_{j_r} \delta(1 - \sum_{l=1}^4 z_l)}{(-\frac{1}{2} z \cdot \mathcal{S} \cdot z)^{3-n/2}} \quad , \\ I_4^{n+4}(j_1) &= \Gamma\left(2 - \frac{n}{2}\right) \\ &\times \int_0^1 \prod_{i=1}^4 dz_i \frac{z_{j_1} \delta(1 - \sum_{l=1}^4 z_l)}{(-\frac{1}{2} z \cdot \mathcal{S} \cdot z)^{2-n/2}} \quad (1) \end{aligned}$$

and scalar integrals  $I_2^n$ ,  $I_3^n$ ,  $I_3^{n+2}$ ,  $I_4^{n+2}$ . We call this basis the GOLEM basis. Note that any  $N$ -point function can be mapped to this basis without introducing inverse Gram determinants, i.e.  $1/\det(G)^r$  with  $G_{ij} = 2r_i \cdot r_j$ ,  $r_j = p_1 + \dots + p_j$ , which occur in Passarino-Veltman reduction. There are three alternatives for evaluating the basis elements:

1. algebraic reduction to the one-loop master integrals  $I_2^n$ ,  $I_3^n$ ,  $I_4^{n+2}$ ,
2. semi-numerical reduction to scalar integrals,
3. direct numerical evaluation.

In this context, semi-numerical means that the same reduction formulas as in 1. are applied at the numerical level. In case 1. and 2. Gram determinants are reintroduced. The direct numerical evaluation is chosen whenever numerically critical phase space regions are approached.

For the numerical evaluation of the GOLEM basis integrals two different methods have been developed. The first is based on contour deformation in Feynman parameter space [7] and the second on performing the Cauchy integration explicitly [11]. The latter method is faster, since (at most) 2- rather than 3-dimensional representations are used. We have tested the robustness of the numerical routines for large samples of realistic phase space points.

The algebraic/numerical algorithms are implemented in the flexible Fortran 90 code GOLEM90.

### 3. Applications to LHC phenomenology

Using the algorithms discussed above, several computations relevant for LHC phenomenology have been carried out so far. We present three examples here, others can be found in [17,18,19].

#### 3.1. The process $gg \rightarrow W^*W^* \rightarrow l\bar{\nu}l'\nu'$

This process contributes to the dominant irreducible background to the Higgs production process  $gg \rightarrow H \rightarrow W^*W^*$ . It is also relevant below the  $WW$  threshold. The gluon-vector boson interaction is mediated by a quark loop. On-shell production results with massless [20] and massive quarks [21] have been known for a long time. For on-shell  $W$  bosons, a phenomenological analysis can be found in [22]. We have now a full calculation for off-shell  $W$ -pairs, where the first two quark generations are treated massless, but the bottom and top masses in the third generation are kept. In the latter case the amplitude contains six different scales: the Mandelstam variables  $s, t$ , the  $W$ -virtualities  $s_3, s_4$  and the quark masses  $m_b, m_t$ . For this amplitude, it is possible to reduce algebraically down to master integrals,  $I_2^n, I_3^n, I_4^{n+2}$ . The amplitude is represented by nine independent gauge-invariant structures. Each coefficient can be written as a linear combination of 27 basis functions. The algebraic simplification results in amplitude representations which have at most one inverse Gram determinant. The Gram determinant is related to the transverse momentum of the  $W$  bosons by  $p_T^2(W) = \det(G)/s^2$ . In this computation there is a tiny phase space region  $p_T(W) < 0.1$  GeV,  $|s_{3,4} - M_W^2| \gg M_W \Gamma_W$  which is numerically problematic, but it does not contribute sizably to the relevant cross sections [23]. In Tab. 1 we show typical LHC cross sections for two massless generations and including the third generation. We also compare to the full NLO result for  $q\bar{q} \rightarrow W^*W^*$ , which is computed using MCFM [24]. Cross sections without selection cuts (tot), with standard LHC cuts (std) and Higgs search cuts (bkg) are given (see [23] for details). This calculation shows that for Higgs search cuts the  $gg \rightarrow W^*W^*$  process enhances the previously known  $W$ -pair background by approximately 30%

	$gg$ (2 gen.)	$gg$ (3 gen.)	$\frac{\sigma_{NLO+\sigma_{gg}}}{\sigma_{NLO}}$
$\sigma_{tot}$	53.61(2)	60.12(7)	1.04
$\sigma_{std}$	25.89(1)	29.79(2)	1.06
$\sigma_{bkg}$	1.385(1)	1.416(3)	1.30

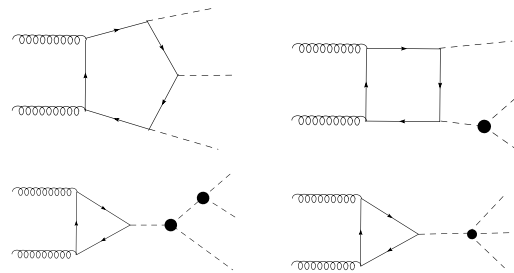
Table 1

Background cross sections in fb for charged lepton pair production in gluon fusion  $gg \rightarrow W^*W^* \rightarrow l\bar{\nu}l'\nu'$ . Results for two and three quark generations are shown for different selection cuts. The last column shows the importance of the gluon fusion process (3 gen.) relative to the quark induced channel in NLO QCD.

and has to be taken into account in experimental studies. In Fig. 1, we show the charged-lepton azimuthal opening angle distribution.

#### 3.2. The process $gg \rightarrow HHH$

Multi-Higgs production via gluon fusion allows in principle to measure the triple and quartic Higgs self-coupling. A full calculation of three Higgs boson production in gluon fusion was accomplished recently by [25]. Four topologies with different sensitivities can be distinguished.



The amplitude can be decomposed into five independent gauge invariant structures  $\text{tr}(\mathcal{F}_1\mathcal{F}_2)$ ,  $p_2 \cdot \mathcal{F}_1 \cdot p_l$ ,  $p_1 \cdot \mathcal{F}_2 \cdot p_j$ ,  $l, j \in \{3, 4\}$ , where  $\mathcal{F}$  is the gluon field strength tensor. Some of the respective coefficients are related by Bose symmetry. Evaluating all coefficients and testing these relations serves as a check of the calculation. Algebraic reduction to 68 master integrals is possible and one finds a numerically stable representation of the amplitude with at most one inverse Gram determinant. The result is summarised in Fig. 2. Destructive interference effects are present between pentagon box and box triangle topologies.

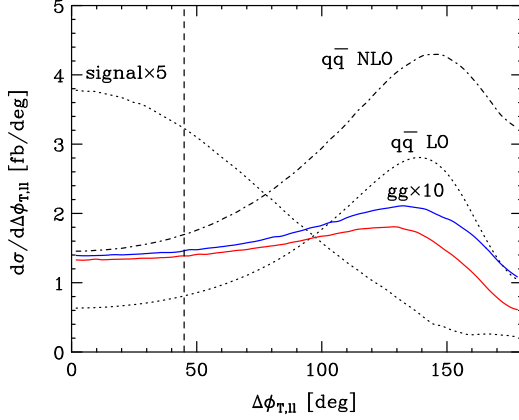


Figure 1. Azimuthal opening angle distribution for the charged lepton pair at the LHC. The upper (lower) solid line is the gluonic contribution ( $\times 10$ ) including (excluding) the massive third family quarks. The other curves are the Higgs signal ( $\times 5$ ) and LO/NLO quark contribution (MCFM). For details see [23].

The total cross section for  $m_H = 120$  GeV, being only of the order of 0.06 fb, is out of reach at the LHC. Note that in Beyond Standard Model scenarios with an enlarged fermion or Higgs sector this cross section could be much larger. We compared our full result to the heavy top limit and observed that for three Higgs boson production the  $m_{top} \rightarrow \infty$  approximation is not applicable. Here, the kinematically favoured region is above the  $2m_{top}$  threshold, rather than below, as required by the heavy top limit.

### 3.3. The $PP \rightarrow 4$ jet amplitude

Up to now no full LHC process with  $2 \rightarrow 4$  kinematics has been evaluated. To have a good theoretical prediction for the huge four jet rate, next-to-leading order corrections to the partonic reactions  $gg \rightarrow gggg$ ,  $gg \rightarrow ggq\bar{q}$ ,  $gg \rightarrow q\bar{q}q\bar{q}$ ,  $q\bar{q} \rightarrow q\bar{q}q\bar{q}$  plus crossings need to be evaluated. By using our GOLEM algorithm we have produced a representation of the six quark amplitude in terms of the GOLEM basis integrals (1) which allows for the semi-numerical evalu-

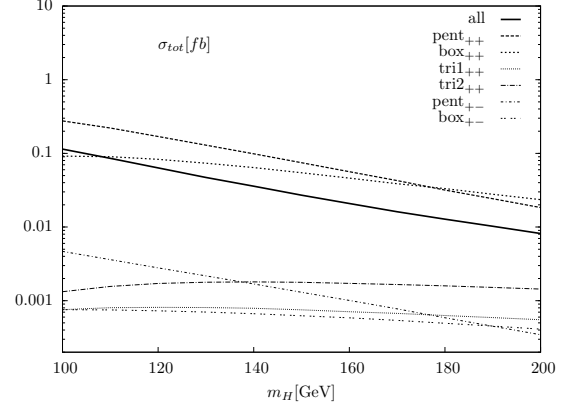
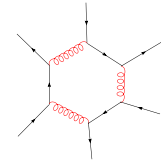


Figure 2. The total triple Higgs production cross section vs.  $m_H$  for different topologies ( $tri1 \sim \lambda_{4H}$ ,  $tri2 \sim \lambda_{3H}^2$ ). The  $+-$  helicity component and all triangle topologies are suppressed.

ation of this amplitude. The evaluation time of one kinematical point is of the order of a second. Alternatively we have produced an algebraic representation of the amplitude in terms of master integrals  $I_2^n$ ,  $I_3^n$  and  $I_4^{n+2}$ . The two independent approaches allow for an efficient debugging of our algebraic/numerical procedures. As this work is not yet completed we just illustrate this by providing a numerical evaluation of the most complicated Feynman diagram in this calculation, the 6-quark pentagon diagram



This diagram can be written as

$$A^{\lambda_1 \lambda_2 \lambda_3 \lambda_4 \lambda_5 \lambda_6}(k_1, \dots, k_6) = \frac{g_s^6}{(4\pi)^2} \frac{1}{s} \left[ \frac{A}{\epsilon^2} + \frac{B}{\epsilon} + C + \mathcal{O}(\epsilon) \right]$$

For the helicity amplitude  $++++++$  and the kinematical point

$k$	$k^0$	$k^1$	$k^2$	$k^3$
$k_1$	7000.	0.	0.	7000.
$k_2$	7000.	0.	0.	-7000.
$k_3$	5105.37	1752.05	-972.19	-4695.74
$k_4$	4582.45	-3465.91	1373.64	2664.47
$k_5$	2917.90	2182.21	876.20	1727.53
$k_6$	1394.27	-468.35	-1277.65	303.74

we find, up to an overall phase,

$$\begin{aligned}
A &= 3.27888 + i 0.950546, \\
B &= 10.7288 + i 15.53100, \\
C &= -1.16693 + i 59.1171.
\end{aligned}$$

The evaluation time for this point with our code is about 0.2 sec on a standard PC (Pentium 4, 2.8 GHz). The evaluation of the full 6-quark amplitude including real emission corrections is in progress.

#### 4. Conclusion

In this talk we presented our GOLEM approach for the evaluation of one-loop multi-leg processes relevant for precise LHC phenomenology. The formalism allows in principle for the evaluation of general  $N$ -point processes with massive and/or massless particles. The algebraic/numerical reduction and evaluation techniques are implemented in the Fortran 90 code **GOLEM90**. As applications, recent results for the gluon-induced processes  $gg \rightarrow W^*W^* \rightarrow l\bar{\nu}l'\nu'$ ,  $gg \rightarrow HHH$  and the hexagon process  $q\bar{q} \rightarrow q\bar{q}q\bar{q}$  were presented.

#### Acknowledgement

T.B. would like to thank the conference organizers for the stimulating conference in Eisenach. The work of T.B., S.K. and N.K. was supported by the Deutsche Forschungsgemeinschaft (DFG) under the grant number Bi1050/1-1.&2. and the Bundesministerium fuer Bildung und Forschung (BMBF) under contract number 05HT1WWA2.

#### REFERENCES

1. C. Buttar *et al.*, arXiv:hep-ph/0604120.
2. V. Buscher and K. Jakobs, Int. J. Mod. Phys. A **20** (2005) 2523 [arXiv:hep-ph/0504099].
3. A. Denner and S. Dittmaier, Nucl. Phys. B **734** (2006) 62.
4. A. Denner, S. Dittmaier, M. Roth and L. H. Wieders, Nucl. Phys. B **724**, 247 (2005).
5. R. K. Ellis, W. T. Giele and G. Zanderighi, Phys. Rev. D **73** (2006) 014027.
6. R. K. Ellis, W. T. Giele and G. Zanderighi, JHEP **0605** (2006) 027.
7. T. Binoth, J. P. Guillet, G. Heinrich, E. Pilon and C. Schubert, JHEP **0510** (2005) 015.
8. A. van Hameren, J. Vollinga and S. Weinzierl, Eur. Phys. J. C **41** (2005) 361.
9. W. T. Giele and E. W. N. Glover, JHEP **0404** (2004) 029.
10. Z. Nagy, D. E. Soper, JHEP **0309** (2003) 055.
11. T. Binoth, G. Heinrich and N. Kauer, Nucl. Phys. B **654** (2003) 277.
12. G. Duplancic and B. Nizic, Eur. Phys. J. C **35** (2004) 105.
13. A. Ferroglia, M. Passera, G. Passarino and S. Uccirati, Nucl. Phys. B **650** (2003) 162.
14. T. Binoth, J. P. Guillet and G. Heinrich, Nucl. Phys. B **572** (2000) 361.
15. J. A. M. Vermaseren, arXiv:math-ph/0010025.
16. A. I. Davydychev, Phys. Lett. B **263**, 107 (1991).
17. T. Binoth, J. P. Guillet, G. Heinrich and C. Schubert, Nucl. Phys. B **615** (2001) 385.
18. T. Binoth, Nucl. Phys. Proc. Suppl. **116** (2003) 387.
19. T. Binoth, J. P. Guillet and F. Mahmoudi, JHEP **0402** (2004) 057.
20. E. W. N. Glover and J. J. van der Bij, Phys. Lett. B **219** (1989) 488.
21. C. Kao and D. A. Dicus, Phys. Rev. D **43** (1991) 1555.
22. M. Duhrssen, K. Jakobs, J. J. van der Bij and P. Marquard, JHEP **0505** (2005) 064.
23. T. Binoth, M. Ciccolini, N. Kauer and M. Krämer, JHEP **0503** (2005) 065. Code for massless case is available at <http://hepsource.sf.net/GG2WW>, update including the massive code in preparation.
24. J. Campbell and R. K. Ellis, Phys. Rev. D **65** (2002) 113007.
25. T. Plehn and M. Rauch, Phys. Rev. D **72**, 053008 (2005).